PERGAMON

Quaternary Science Reviews 22 (2003) 1647–1658

QSR

Simulation of atmospheric radiocarbon during abrupt oceanic circulation changes: trying to reconcile models and reconstructions

Gilles Delaygue*, Thomas F. Stocker, Fortunat Joos, Gian-Kasper Plattner

Climate and Environmental Physics (KUP), Physics Institute, University of Bern, Sidlerstrasse 5, CH-3012 Bern, Switzerland

Received 10 July 2002; accepted 22 May 2003

Abstract

An abrupt increase in the atmospheric ^{14}C content at the beginning of the Younger Dryas, about 13,000 years ago, has been related to a slow-down of the global oceanic circulation. This has been well simulated by box models, but the amplitude and timing of such a ^{14}C change could not be represented with dynamical models. We have forced a climate model of intermediate complexity with a meltwater discharge to test three model parameters that have the potential to strongly influence the simulated ^{14}C change and may help us to reconcile the model results with reconstructions. We find that a decrease of the tropical wind speed accompanying a slow-down of the oceanic circulation largely amplifies the circulation-induced ^{14}C change and brings it closer to the reconstructions. Second, we find that vertical mixing in a dynamical ocean model leads to a substantial damping in the ^{14}C response of simple models. Third, we demonstrate that neglecting radiocarbon 'reservoir age' variations during abrupt climate change may lead to a substantial overestimate of atmospheric ^{14}C fluctuations reconstructed from paleoceanographic archives.

1. Introduction

The last deglaciation happened in two steps in the north Atlantic basin, with an intermediate return to cold conditions, nearly as cold as those prevailing during glacial times (e.g., Broecker et al., 1985; Jouzel et al., 1995). The origin of this cold return, the Younger Dryas, is still debated. Different paleo-records and modelling studies point to a break-down of the oceanic 'conveyor belt', responsible for a large part of the heat transport from low to high latitudes in the Atlantic basin (see Clark et al., 2002, for a review). Two pieces of evidence support this hypothesis.

First, the deglaciation was accompanied by a meltwater discharge from the ice sheets to the northern Atlantic, which may have triggered the collapse of the north Atlantic deep overturning and, as a consequence, a large climatic change (Stocker and Wright, 1991; Manabe and Stouffer, 1995).

Second, the ^{14}C content of the atmosphere, as reconstructed from oceanic and lake sediments, displays a large and rapid increase at the onset of the Younger Dryas, of about 70‰ over 200 years as reconstructed from the Cariaco Basin (Hughen et al., 2000). This important change may be caused by a large decrease in the surface-to-deep ocean exchange, isolating the atmosphere from the ocean, and increasing the ^{14}C content of the atmosphere where the ^{14}C is produced (Siegenthaler et al., 1980). A break-down of the global 'thermohaline' circulation, which reduces the vertical exchange in the ocean, is thus qualitatively consistent with the observed ^{14}C increase (Stocker and Wright, 1996). Simple models like box models, in which the ocean circulation is prescribed, succeed in reproducing this ^{14}C increase. However, models calculating the ocean circulation from the temperature and salinity fields, so-called 'dynamical models', have failed to quantitatively reproduce this ^{14}C variations (Mikolajewicz, 1996; Broecker, 1998; Marchal et al., 2001: dashed line in their Fig. 1a). In particular, the simulated atmospheric ^{14}C change: (i) is consistently too small (up to 30‰ at most compared to more than 70‰ estimated by Hughen et al., 2000); (ii) increases too slowly (within ~1000 years compared to ~200 years in reconstructions); (iii) decreases only after

*Corresponding author. Current address: CEREGE, Europôle de l'Arbois BP80, 13545 Aix-en-Provence, Cedex 4, France. Tel.: +33-4-42-97-15-33; fax: +33-4-42-97-15-95.

E-mail address: delaygue@cerege.fr (G. Delaygue).

0277-3791/03/$ - see front matter © 2003 Elsevier Ltd. All rights reserved.
doi:10.1016/S0277-3791(03)00171-9

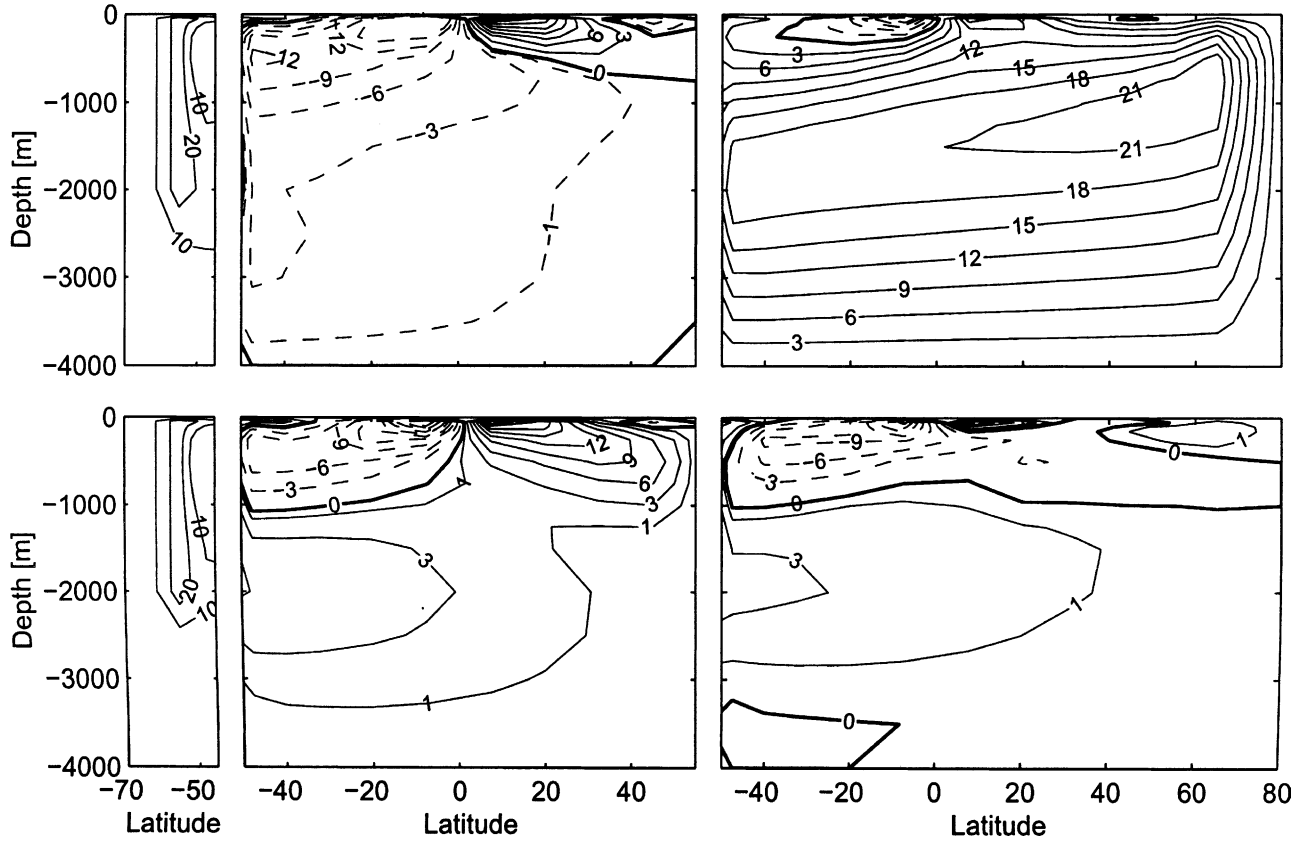

Fig. 1. Simulated oceanic overturning (stream function in Sverdrups $\equiv 10^6\,m^3/s$) for the Southern Ocean (left panels), the Pacific (middle panels) and the Atlantic (right panels), at two different times: at steady state (after 16 kyr, ie., $t=0$; upper panels); and after the meltwater peak ($t=600$ years; lower panels). Positive values (solid lines) represent a clockwise circulation; negative values (dashed lines) a counterclockwise circulation. The zero line is bold. The deep overturning in the Atlantic (> 1000 m) collapses from a maximum of 23 Sv to less than 5 Sv.

the full recovery of the oceanic circulation (whereas in the reconstructions the ^{14}C decrease started in the middle of the Younger Dryas) (Table 1). Only part of these variations may be attributed to changes in the atmospheric production of ^{14}C. A production history reconstructed by Muscheler et al. (2000) shows variations qualitatively in line with the atmospheric ^{14}C values but too limited in amplitude, even when contributions due to changes in the ocean circulation are added (Marchal et al., 2001). However, Marchal et al. (2001) pointed out that the production estimated by Muscheler et al. (2000) does not contain the long-term negative trend common to all cosmogenic nuclides over the last deglaciation (e.g., Bard, 1998). Hence, it is not clear how reliable this production history is, neither which role this production actually played in the ^{14}C fluctuations.

Here, we try to reconcile a collapse of the oceanic circulation with the observed ^{14}C change using a dynamical ocean model in which we adjust three model parameters likely to have a large impact and not previously studied with a dynamical model: (i) the meltwater discharge, which influences the rate of ocean circulation change; (ii) the wind stress, which partly controls the ^{14}C exchange between the atmosphere and the ocean; (iii) the oceanic vertical diffusivity, which controls the vertical mixing of ^{14}C within the ocean and influences the circulation itself. We focus on the sharp ^{14}C increase at the beginning of the Younger Dryas, which is the less explained feature of the ^{14}C variations.

2. Model description

We use a zonally averaged, dynamical ocean model, with three connected basins, coupled to an energy balance model of the atmosphere and a thermodynamical sea-ice model (Stocker and Wright, 1996). There are 14 vertical levels in the 4000 m deep ocean, including a 50 m thick surface mixed layer. Tracers are transported by convection, advection and diffusion, the latter process representing the Eddy transport not explicitly resolved in the model. The vertical diffusivity K_v is set to $2\times10^{-5}\,m^2/s$. A closure parameter ε, relating the east–west pressure difference to north–south pressure gradients, is set to 0.4 (Stocker et al., 1992). A high salinity (35.6) is prescribed in the northern-most box of the Atlantic in order to simulate a realistic circulation,

Table 1
Comparison of the initial atmospheric $\Delta^{14}C$ increase between reconstruction and simulations

Data type for the atmospheric $\Delta^{14}C$	Amplitude and duration of increase	Level 500 years after the beginning of the discharge	Maximum increase rate over a 200-year period
Detrended reconstruction by Hughen et al. (2000)	~70‰ over 200 yr ~100‰ over 1000 yr	[a]	70‰/200 yr
Standard simulation (Fig. 2)	37‰ over 1500 yr	9‰	14‰/200 yr
Simulation with instantaneous discharge (Fig. 2)	41‰ over 1400 yr	24‰	12‰/200 yr
Simulation with tropical wind stress decreased by 50% (Fig. 3)	55‰ over 1100 yr	32‰	20‰/200 yr
As above but reconstructed from the tropical Atlantic without accounting for reservoir age changes (Fig. 7)	77‰ over 1100 yr	56‰	35‰/200 yr
Simulation with $K_v = 5 \times 10^{-6}\,m^2/s$ for the ^{14}C tracer (Fig. 4)	46‰ over 1500 yr	10‰	16‰/200 yr

[a] Already decreasing 500 years after the onset of the Younger Dryas; ~30‰ 500 years after the start of the increase (around 13.5 kyr BP).

with a maximum deep overturning of ~23 Sv (1 Sverdrup$\equiv 10^6\,m^3/s$) in the Atlantic basin (Fig. 1). The atmospheric hydrological cycle implemented by Schmittner et al. (2000) permits meridional transport of water vapour both by diffusion and advection.

We use the carbon model described by Siegenthaler et al. (1980), in which the carbon inventories and the fluxes between the different reservoirs (atmosphere, ocean, and terrestrial biosphere) are kept constant. Accounting for the slight increase of atmospheric CO_2 recorded over the Younger Dryas has a very small effect on the ^{14}C tracer in this model (Marchal et al., 1999). Following Toggweiler et al. (1989), the ^{14}C tracer is simulated as the relative change to the steady state ^{14}C atmospheric concentration (arbitrarily set to 1), and expressed in permil as $\Delta^{14}C = (^{14}C - 1) \times 1000$, which then compares with the $\Delta^{14}C$ defined by Stuiver and Polach (1977). The ^{14}C fluxes are thus only due to ^{14}C gradients and to the radioactive decay.

The coupled model is first spun-up to a dynamical quasi-steady state over 15,000 years (15 kyr). An atmospheric ^{14}C value of 1 ($\Delta^{14}C = 0$‰) is prescribed during this spin-up in order to reach a ^{14}C steady state in the different reservoirs. After this spin-up, the atmospheric production of ^{14}C is diagnosed so as to exactly balance the global decay. This production is kept constant in further simulations. At this point, the atmospheric ^{14}C is allowed to freely evolve, and the simulation is continued for another kyr to test the ^{14}C budget: a perfect steady state is not reached, which is evidenced by a slight but negligible $\Delta^{14}C$ drift in the atmosphere from the ideal value of 0‰ (typically 5×10^{-3} ‰/kyr). In this quasi-steady state, the mean oceanic $\Delta^{14}C$ is −160‰ (−50‰ in the oceanic mixed layer). This point of the simulation, after 16 kyr of spin-up, constitutes the start of all the simulations presented in the following, and marks the time $t = 0$. In the next section, we describe the standard simulation with a meltwater discharge, which serves as a reference for the sensitivity simulations presented in Sections 4–6.

3. Simulated $\Delta^{14}C$ variations during a meltwater discharge

A meltwater discharge is prescribed in the north Atlantic (ca 40°N). We use a triangular shape in time (Fig. 2), an approximation of the profile inferred by Fairbanks (1989). A volume corresponding approximately to twice MWP-IA ($14 \times 10^{15}\,m^3$) spread over

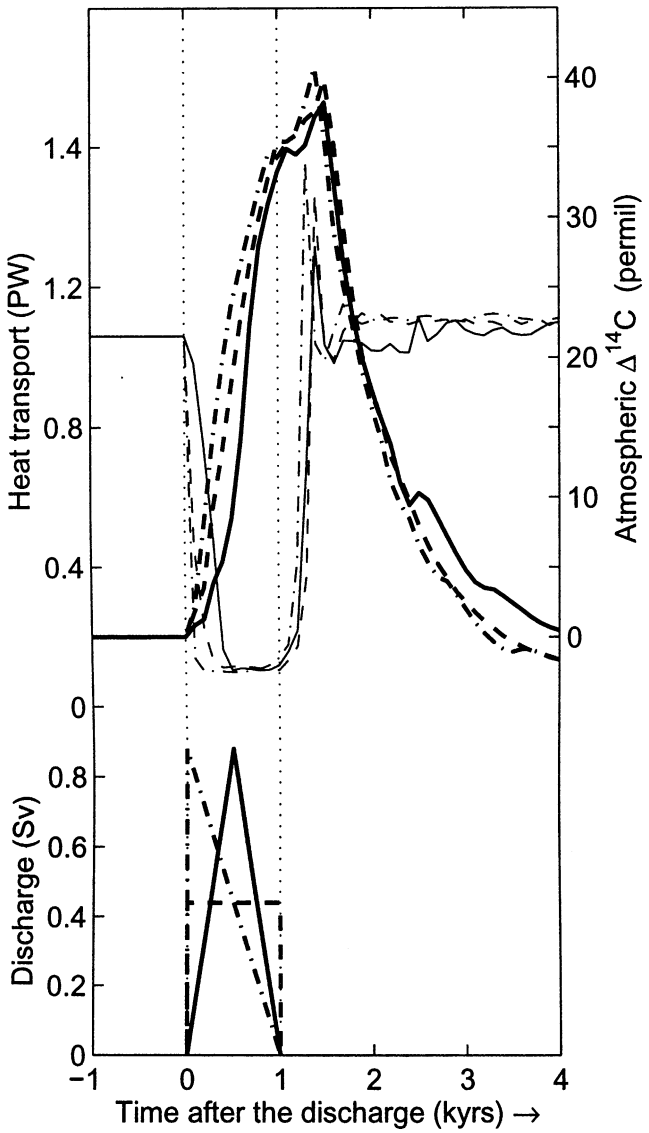

Fig. 2. Simulated changes of (i) the maximum northward heat transport by the Atlantic (thin lines), in petawatts ($1\,PW = 10^{15}\,W$) and (ii) the atmospheric $\Delta^{14}C$ response (bold curves in the upper part), in response to different meltwater discharge histories of $14 \cdot 10^{15}\,m^3$ in total (bold curves in the lower part, in Sverdrups). In our standard setup (solid curves), the discharge rate follows a triangular shape, peaking at 0.88 Sv. The northward transport of heat by the Atlantic drops from a maximum of 1.1 PW to less than 0.2 PW. In two alternative scenarios (dashed and dot-dashed curves), the rate increases to its maximum instantaneously, and is then constant or decreases.

1000 years is needed to simulate a collapse of the heat transport by the north Atlantic as well as climatic changes at northern latitudes in line with observed ones.

The response of the model to this meltwater discharge is a collapse of the deep overturning (Fig. 1) and northward transport of heat (Fig. 2) in the Atlantic Ocean within less than 500 years. This shutdown is associated with a shallowing of the deep convection in the northern Atlantic from ~1300 m to less than 200 m. The deep overturning in the Pacific stays weak (<6 Sv), but reverses from a counterclockwise to a clockwise circulation in Fig. 1 (left panels), associated with a doubling of the convection depth in the northern part (500 to 1000 m). This reversal increases the ventilation of the intermediate waters (down to ~2000 m) in the Pacific, especially in the northern part. The deep convection activity in the Southern Ocean decreases slightly, due to a reduction in the intermediate salty water inflow from the north Atlantic, but a parameterization of brines, simulating the formation of seasonal sea ice around Antarctica (Stocker and Wright, 1996), keeps the Southern Ocean well ventilated.

During this meltwater discharge, the atmospheric $\Delta^{14}C$ increases by up to 35–40‰ (Fig. 2), before returning to its steady-state value after the end of the discharge. As a whole, this increase is due to a drop of the deep ocean ventilation, which depletes the deep ocean in ^{14}C compared to the steady state, and enriches the ocean surface and atmosphere, where the ^{14}C production is kept constant (see also Section 6 and Fig. 6). This corresponds to the drop in the deep Atlantic overturning over the first ~500 years. Yet, the slight increase in the ventilation of the intermediate north Pacific limits this atmospheric ^{14}C increase. This latter dynamical response has been simulated with similar scenarios (e.g., Mikolajewicz et al., 1997; Seidov and Haupt, 1997), and matches interpretation of geological records from the Younger Dryas (Duplessy et al., 1989; van Geen et al., 1996). Thus, the response of a dynamical model to a freshwater discharge is not spatially homogeneous, and may not be equivalent to globally reducing the vertical exchange in the ocean. We now modify three model parameters in the aim to obtain a ^{14}C response closer to the observed one, namely the rate of the freshwater discharge, the wind speed, and the vertical diffusivity.

4. Sensitivity of $\Delta^{14}C$ to the meltwater discharge

We use a triangular shape for the meltwater discharge rate (Fig. 2), approximating the bell-shaped curve inferred by Fairbanks (1989) from the sea level step MWP-IA. This assumes a rather long delay until the maximum rate is reached. Recent reconstructions, however, suggest a possibly much more rapid onset of the discharge (Clark et al., 2001). Barber et al. (1999) proposed that the drainage of the peri-glacial lakes surrounding the Laurentide ice sheet, about 8,200 years ago, happened in less than 1 year, based on a simulation of sediment deposition. Björck (1995) described the drainage of the Baltic sea during the last deglaciation as short events lasting ~10 years. The rate of the discharge is likely to influence the vertical stability in the northern Atlantic, which depends on the interplay between the surface freshening (less dense than the underlying water)

and the efficiency of mixing processes to dilute this freshwater.

We have tried different discharge patterns, for the same volume of meltwater (Fig. 2). In the extreme case of an instantaneous discharge, the ^{14}C response in the atmosphere starts earlier, but the rate is not faster and the maximum not higher than in the standard case (Table 1). Doubling the volume of the discharge results in a more rapid $\Delta^{14}C$ increase but also extends the $\Delta^{14}C$ positive anomaly in time, in contrast to the geological reconstructions (not shown).

An alternative way to alter the vertical exchange in the ocean is to modify the wind, which partly controls the oceanic circulation and the atmosphere-ocean ^{14}C exchange.

5. Sensitivity of $\Delta^{14}C$ to zonal wind

Wind is the principal driver of surface ocean circulation, and strongly dominates vertical displacements in the top few hundred meters due to Ekman transport. It also controls the air–sea flux of gases, thus the ^{14}C net flux to the ocean.

In our scenarios of abrupt climate change, which are based on the collapse of the THC, sea surface temperatures and gradients and ocean-to-atmosphere heat fluxes will change. This has an effect on the atmospheric circulation and hence on wind speed. In our standard model setup, the wind stress, the force which affects the ocean surface, is prescribed from present-day values and kept constant. We have tested the importance of wind stress variations for the atmospheric ^{14}C.

An estimation of the wind changes during the Younger Dryas proves difficult even qualitatively, because of the ambiguity of geological records. For instance, the higher flux of dust inferred from sediments can be ascribed to stronger wind, or alternatively to larger dust source areas. Also, the oceanic equatorial productivity may be related to the intensity of the upwelling, and thus of the trade winds, but the sign of its variation during cold climates is still in debate (see Loubere, 1999, for a review). Still, a consensus seems to exist regarding stronger winds at mid-to-high latitudes, an expected response given the stronger meridional temperature gradient. Simulations of Younger Dryas-type events have been conducted with coupled general circulation models (GCMs) by prescribing a meltwater discharge, and they provide consistent estimates regarding the geographical and temporal changes of wind stress (Manabe and Stouffer, 1997; Schiller et al., 1997; Rind et al., 2001; Vellinga and Wood, 2001). Similar simulations have related the wind change to its geostrophic component (Fanning and Weaver, 1997) or to climatic parameters through empirical relationships (Mikolajewicz, 1996). A common response of these simulations is a strengthening of the zonal winds at mid-latitudes, especially over the Southern Ocean. A less marked feature, but also common to some of these simulations, is a weakening of the wind in the intertropical region, a clear response in the simulation of Rind et al. (2001, Fig. 9). Schiller et al. (1997) found a weakening of the trade winds in the southern hemisphere and a strengthening in the northern, in relation with the changing Hadley cell intensity. Vellinga and Wood (2001) reported a consistent weakening of the zonal wind in the tropical west Pacific, Indian and south Atlantic (by at least 10–20%), but stronger tropical winds in the east Pacific and Atlantic. Such a weakening of the tropical wind speed is not inconsistent with productivity changes estimated from geological records for the Younger Dryas or at least for glacial periods (e.g., Beaufort et al., 2001, for the west Pacific; Loubere, 1999, for the east Pacific; Marcantonio et al., 2001, for the Indian Ocean).

In a straightforward test, without any meltwater discharge, we halved the Easterlies' wind stress (20°S to 32°N), which increased the atmospheric $\Delta^{14}C$ by 23‰ at equilibrium (not shown). Inspection of the oceanic $\Delta^{14}C$ change shows a globally averaged depletion between $\sim$500 and 2500 m by 2‰, with the strongest change (depletion of 80‰) taking place around 500 m in the north Pacific, associated with a reduction of the deep convection. This reduction is due to a strong freshening of the surface, by 1 to 2 units of salinity. A similar simulation in which the precipitation-minus-evaporation budget was kept locally constant showed a salinity decrease of only $\sim$0.2, and a very limited atmospheric $\Delta^{14}C$ increase (2–3‰). This suggests that reducing the Easterlies decreases the vertical exchange in the ocean (hence increasing the atmospheric $\Delta^{14}C$) not so much at the Equator (equatorial upwelling) but also at high latitudes, via the hydrological cycle.

In a similar simulation, again without discharge, we doubled the wind stress at mid-to-high latitudes in both hemispheres (55°S–32°S, 45°N–55°N), and obtained the opposite response: a $\sim$10‰ drawdown of the atmospheric $\Delta^{14}C$, due to an increased overturning in the Southern and Atlantic Oceans (not shown). We performed similar simulations which consistently showed that decreasing the wind stress enriches the atmosphere in ^{14}C, and conversely. Thus, an increase of the wind stress at mid-latitudes and a decrease at low latitudes, which may be expected following a meltwater discharge (see discussion above), have opposite effects on the atmospheric $\Delta^{14}C$.

To test the effect of associating such a wind change to a meltwater discharge, we simply synchronized the wind change with the meridional Atlantic heat transport (Fig. 2) through a linear relationship. The rationale of this synchronisation is that the zonal wind is related to some gradient of surface temperature, as for the heat

transport (e.g., Rind, 1998). The results are summarised in Fig. 3. A 50% change in the tropical wind stress amplifies the atmospheric $\Delta^{14}C$ response, by almost 20‰, sharpens its initial increase, and provokes an earlier drawdown, by almost 500 years. All these changes bring the atmospheric $\Delta^{14}C$ response closer to the reconstructed values. The effect on the oceanic $\Delta^{14}C$ is strongest at intermediate depth in the northern Pacific. These simulations confirm the sensitivity of the atmospheric $\Delta^{14}C$ to the zonal wind described above (in the simulations without discharge), but they also underline the importance of coupling oceanic circulation and wind stress: for instance, the increase of the tropical Easterlies at the end of the meltwater discharge helps the thermohaline circulation to recover, which explains the earlier drawdown of the atmospheric $\Delta^{14}C$ compared to the standard simulation with constant wind.

A change in the wind stress, implying a change in the wind speed, has also some consequence on the air–sea gas exchange. In our standard model setup, the exchange coefficient (piston velocity) is constant in time and space, equal to 8.3 m/yr. We allowed it to change with the wind speed, using a wind field consistent with the wind stress (Esbensen and Kushnir, 1981), and the formulation of the piston velocity related to long-term wind by Wanninkhof (1992). Changes in the air–sea gas exchange slightly amplify the ^{14}C variations due to the oceanic circulation: for instance, the atmospheric $\Delta^{14}C$ increase due to weaker tropical winds (plain curve in Fig. 3) is now stronger because of a weaker air–sea exchange, but this additional effect is limited, around $\sim$5‰ (not shown).

The atmospheric $\Delta^{14}C$ response to a meltwater discharge appears quite sensitive to a coupled change in the wind stress. A coupled decrease of the tropical wind stress by 50% (plain solid curve in Fig. 3) allows us to simulate a three time faster $\Delta^{14}C$ initial increase ($\sim$25‰ over the first 500 years, compared to 8‰ in the standard simulation), with a maximum value higher by a factor 1.5 (55‰ compared to 37‰, Table 1). Compared to paleo-reconstructions, the rate of initial increase is still considerably weaker by a factor 3–4, and the $\Delta^{14}C$ maximum value is only reached by the end of the discharge, i.e., 1000 years after it starts. To get closer to these reconstructions, the vertical exchange in our ocean model must be globally decreased during the slow-down circulation. Since part of the vertical exchange is achieved in the model by the vertical diffusivity, we now test this parameter.

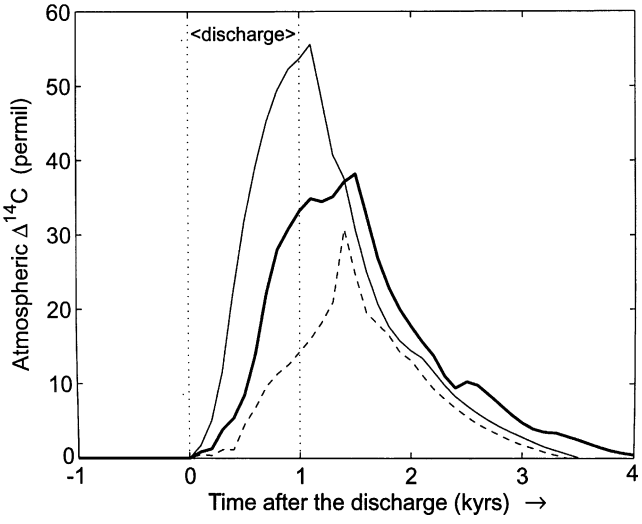

Fig. 3. Sensitivity of the atmospheric $\Delta^{14}C$ response to the wind stress during a meltwater discharge. The bold curve is the standard case with constant wind stress. The two other curves correspond to the ^{14}C response while synchronising wind and circulation changes. In one case (plain curve), the tropical Easterlies (20°S to 32°N) are allowed to change proportionally to the meridional heat transport in the Atlantic, thus decreasing (by approximately a factor of two) during the period with a sluggish circulation (Fig. 2). In the other case (dashed curve), the mid-high latitude wind stress (55°S to 32°S, and 45°N to 55°N) is allowed to change inversely to the same heat transport, thus increasing (by approximately a factor of two) over the period with a sluggish circulation.

6. Sensitivity of $\Delta^{14}C$ to the vertical diffusivity

The atmospheric $\Delta^{14}C$ increase due to the slow-down of the oceanic circulation is globally due to the decoupling between the ocean surface, in equilibrium with the atmosphere where ^{14}C is produced, and the deep ocean, more and more depleted in ^{14}C by radioactive decay. The vertical diffusion in an ocean model, which is the usual parameterization of small-scale processes, acts against this decoupling (Siegenthaler et al., 1980). Coarse resolution ocean models, like ours and the one used by Mikolajewicz (1996), are generally strongly diffusive and therefore may underestimate the decoupling between the surface and the deep ocean, limiting the simulated atmospheric $\Delta^{14}C$ increase associated with a freshwater discharge. In our standard model setup, the ^{14}C vertical diffusivity K_v is constant with depth and latitude, and equals $2\times10^{-5}\,m^2/s$. We varied this standard value, only for ^{14}C, over almost three orders of magnitude, to test whether a weaker vertical diffusivity would translate into a significantly higher atmospheric $\Delta^{14}C$ peak associated with the meltwater discharge. We find that decreasing the vertical diffusivity consistently amplifies the atmospheric $\Delta^{14}C$ response (circles in Fig. 4), but also delays its peak (not shown): between the weaker and stronger values of K_v, the $\Delta^{14}C$ maximum differs by $\sim$45‰ and its delay by more than 600 years.

In these simulations, we have only changed the ^{14}C vertical diffusivity. But there is no reason to use a different diffusivity value for the other tracers, salinity and temperature, and indeed the same value is usually

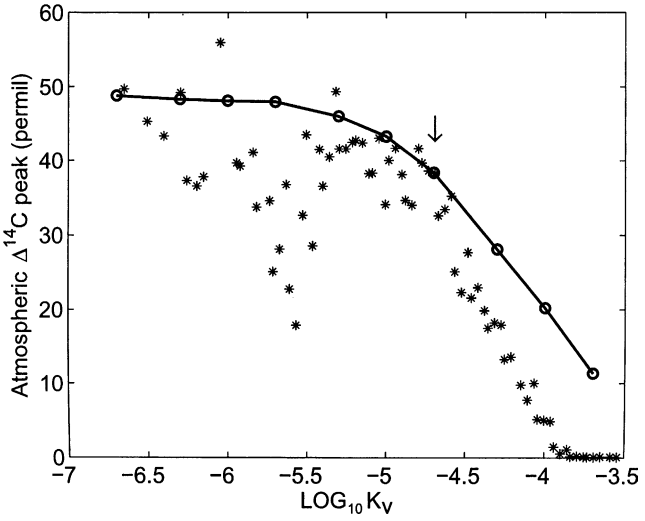

Fig. 4. Sensitivity of the maximum atmospheric $\Delta^{14}C$ response, during a meltwater experiment, to the vertical diffusivity (K_v, expressed here with its base 10 logarithm). The bold line represents results obtained by changing K_v only for the ^{14}C tracer; the stars by changing K_v for all tracers (trying to keep approximately the same steady-state circulation by adjusting the closure parameter ε). The arrow represents the standard case, with a value for K_v of $2 \cdot 10^{-5}\,m^2/s$.

applied for all tracers in ocean models. We thus have changed the diffusivity K_v for all tracers (^{14}C, salinity, and temperature). Because the oceanic circulation itself is strongly dependent on K_v (Wright and Stocker, 1992), this modifies the response of the circulation to the meltwater discharge: the atmospheric ^{14}C sensitivity to K_v thus comprises the effect on the circulation. Because we wanted to compare the ^{14}C response with other models, which usually share a similar steady state circulation, we have adjusted the closure parameter ε of the model so as to simulate approximately the same steady state circulation (*prior* to the meltwater discharge). A similar sensitivity of the $\Delta^{14}C$ response to K_v is found (stars in Fig. 4), but with a strong noise due to fluctuations in the circulation. This suggests that the sensitivity of the ^{14}C response to K_v is well captured by only changing the ^{14}C diffusivity.

The maximum logarithmic sensitivity of the atmospheric $\Delta^{14}C$ to K_v, $(d\Delta^{14}C/\Delta^{14}C)/(dK_v/K_v)$, is found to be -0.011 in our two-dimensional (2D) model (for K_v ranging between 2×10^{-4} and $2 \times 10^{-5}\,m^2/s$, Fig. 4). This is one order of magnitude smaller than the value of -0.11 reported by Siegenthaler et al. (1980) for a 1D box-diffusion model. However, diffusivity coefficients applied in 1D box-diffusion models are not directly comparable to diffusivity coefficients in spatially resolved dynamical models (Joos et al., 1997). The vertical transport of ^{14}C in our 2D model results from the combination of advection, convection, and diffusion, whereas this vertical transport in a box-diffusion model is represented by diffusion only. This may explain why the sensitivity found here is significantly weaker than in the 1D model.

This sensitivity becomes very small for diffusivities lower than $\sim 10^{-6}\,m^2/s$ (Fig. 4). This value represents a minimum for the 'apparent' diffusivity of the global ocean, due to the transport of ^{14}C by the advective and convective activities remaining during the slow-down of the circulation. (Note that an additional transport is generated by the advective scheme, called 'numerical diffusion', but it is partly corrected for, and is found negligible compared to advection and convection.) If, in the past, the real ocean has always had a minimum 'apparent' diffusivity, this should be accounted for in simulations using 1D diffusive or box model. In such models, a collapse of the oceanic circulation is simulated by a strong decrease in the vertical diffusivity or in the mass flux between boxes (e.g., a shut off of the Atlantic overturning, as in Hughen et al., 2000). If the ocean model 'apparent' diffusivity is decreased below the real minimum, the resulting increase in the atmospheric $\Delta^{14}C$ would be substantially overestimated.

In conclusion, decreasing the vertical diffusivity results in a larger, but delayed, peak response in the atmospheric $\Delta^{14}C$. Hence, adjusting the diffusivity alone is not sufficient, in our simulations, to get closer to the reconstructed $\Delta^{14}C$ variations. Nevertheless, the rather strong diffusivity of different models, including ours, may help explain the limited $\Delta^{14}C$ response to a freshwater discharge.

7. Influence on the surface reservoir age

The reconstruction of atmospheric $\Delta^{14}C$ from sediments is based on cross-dating the remains of organisms (which grew in the surface layer) by the ^{14}C technique and by another technique which gives true ages (e.g., varve counting). The difference between both ages is directly related to the $\Delta^{14}C$ of the oceanic surface, and thus to the atmospheric $\Delta^{14}C$ provided that the $\Delta^{14}C$ difference between the surface of the ocean and the atmosphere has remained constant in time. This atmosphere-sea surface $\Delta^{14}C$ difference is usually expressed as an apparent ^{14}C age of the surface called the 'reservoir age' $RA = 8267 \log[(1+\Delta^{14}Catm/1000)/(1+\Delta^{14}Coc/1000)]$ (in years), where $\Delta^{14}Catm$ stands for the atmospheric $\Delta^{14}C$ and $\Delta^{14}Coc$ for the surface oceanic $\Delta^{14}C$ (in permil). Any change in this reservoir age not accounted for when calculating the atmospheric $\Delta^{14}C$ would bias this reconstruction. Hughen et al. (2000) assumed a constant reservoir age in the Cariaco basin in order to determine the atmospheric $\Delta^{14}C$ variation during the Younger Dryas. They based this assumption on the comparison with tree-ring reconstructions of $\Delta^{14}C$ going back to the end of the Younger Dryas. However, other evidence suggests that the

reservoir age in the Atlantic may have strongly and abruptly changed over the last deglaciation (Bard et al., 1994; Siani et al., 2001; Waelbroeck et al., 2001).

We have calculated the reservoir age of the oceanic surface in our simulations. Changes by 200 years, corresponding to a change in air–sea $\Delta^{14}C$ difference by ~25‰, are not uncommon, and the maximum variations (of more than 400 years) are found in the northern Atlantic. Fig. 5 illustrates some typical changes. In the northern Atlantic (Fig. 5a), an abrupt increase by 400–500 years takes place when the deep convection recovers and brings up very old waters to the surface (Fig. 6b; see also Stocker and Wright, 1996, for more details). The abruptness is related to the recovery of the convection ('overshoot', see Fig. 2). In the tropical Atlantic (Fig. 5b), the surface is rejuvenated by ~200 years due to the collapse of the Atlantic overturning, which decreases the flow of aged waters originating from the deep south Atlantic (Fig. 1, right panels). The re-establishment of the circulation advects even older waters from the deep ocean (Fig. 6b). In the equatorial Pacific (Fig. 5c), the surface is rejuvenated by ~200 years during the discharge. This is associated with the reversal of the Pacific deep overturning (Fig. 1, middle panels), which ventilates the equatorial region with intermediate waters originating from the northern part, instead of old deep waters coming through the Southern Ocean. The consistency between the different simulations suggests that the simulated reservoir age variations are rather robust.

These different variations in the reservoir age imply that the sea surface $\Delta^{14}C$ is also strongly influenced by the circulation, and not just a function of the atmospheric $\Delta^{14}C$. Fig. 6 shows the simulated ^{14}C age gradient of the water at steady state and at the end of the discharge (after 1 kyr). This is precisely the surface-to-depth ^{14}C age difference, setting an age of 0 to the surface boxes, as it can be reconstructed from contemporaneous planktic and benthic Foraminifera. Hence, it is not exactly a 'ventilation age' of the ocean, because it does not account for the origin of the water masses (Adkins and Boyle, 1997). The very old deep ages (>2 kyr in the Atlantic, >3 kyr in the Pacific) illustrate the dynamical decoupling between the upper and lower parts of the ocean, associated with the drop in the global circulation, as already shown by Stocker and Wright (1996). This explains the increase in the surface reservoir age at the recovery of the circulation, when old deep waters are advected up to the surface, as shown in Fig. 5. On the contrary, the $\Delta^{14}C$ of the upper 1000–1500 m is closer to the atmospheric $\Delta^{14}C$, so that the vertical gradient of $\Delta^{14}C$ is weaker in the upper ocean. The vertical gradient of ^{14}C age modelled here can be directly compared with ^{14}C dates on contemporaneous organisms (like Foraminifera) living at different depths. Duplessy et al. (1989) presented measurements from the

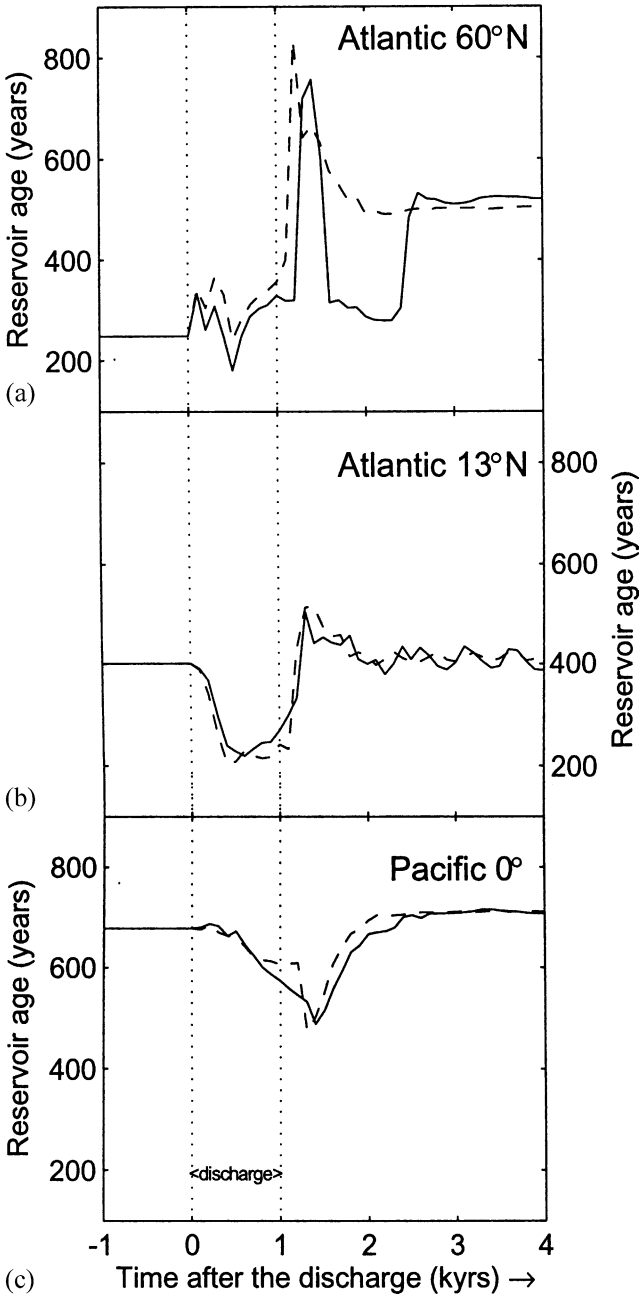

Fig. 5. Simulated surface reservoir age (see text for definition) at three different locations and for three different simulations: (a) northern Atlantic (60°N), (b) tropical Atlantic (13°N) and (c) equatorial Pacific. Full line, standard simulation (bold line in Fig. 3); dashed line, tropical wind stress allowed to decrease by 50% (plain line in Fig. 3).

north Pacific, over the last deglaciation, which show a decrease of this age difference at ~1000 m during the Younger Dryas, consistent with our results (Figs. 6c and d). Broecker et al. (1990) reported some ^{14}C measurements from the deep Atlantic and Pacific for the Last Glacial period, with age differences that are much lower than in our simulations, possibly reflecting a less sluggish circulation during glacial periods than during the Younger Dryas.

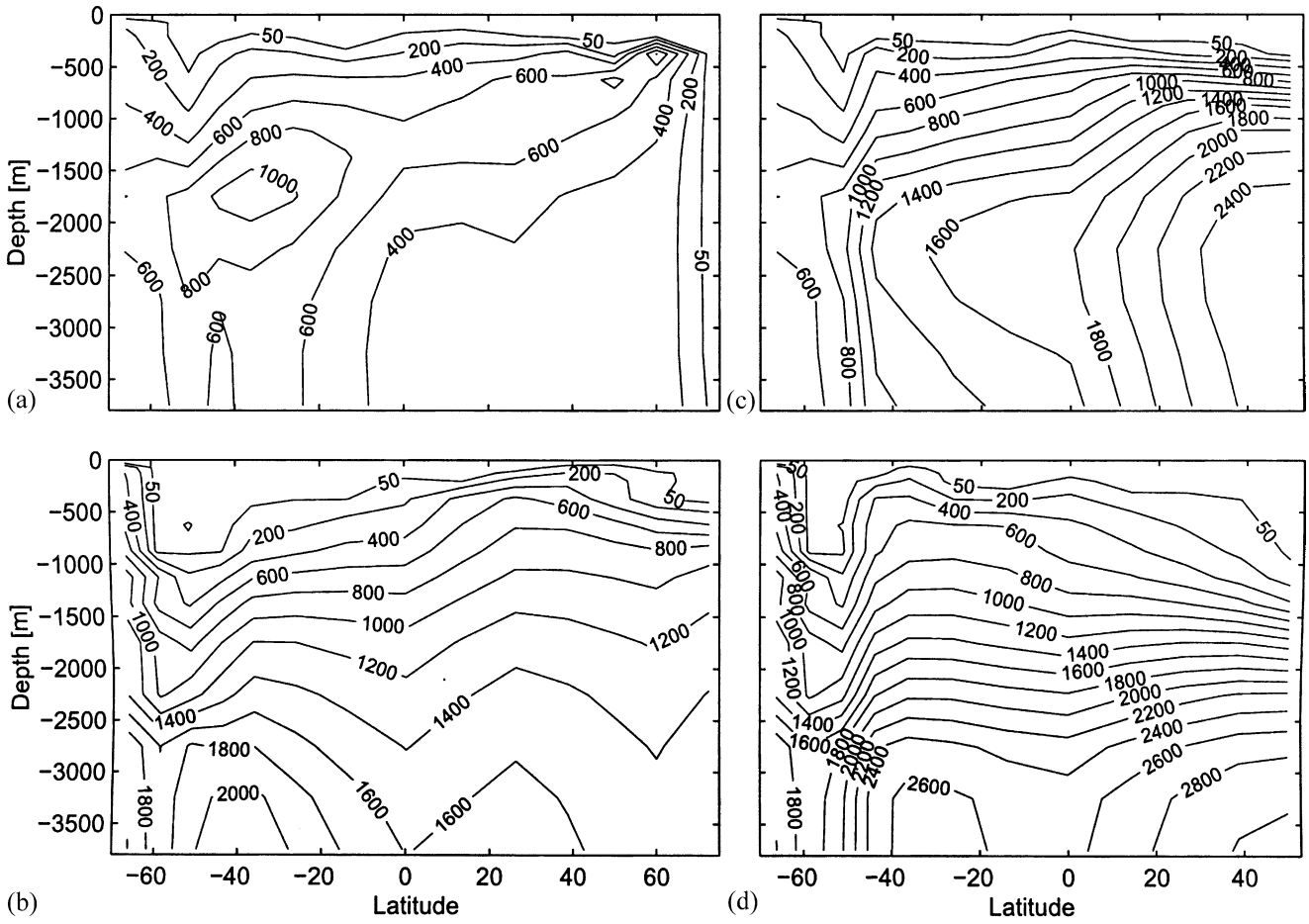

Fig. 6. Simulated ^{14}C age difference between the surface and depth z in the same water column, for two time steps: at steady state (upper panels a and c), corresponding to the modern circulation, and the anomaly after 1 kyr at the end of the discharge (lower panels b and d), just before the circulation recovers. Atlantic Ocean: left panels a and b; Pacific Ocean: right panels c and d. This age difference is calculated for each box as (in years):

$$8267 \log[(1 + \Delta^{14}C_S/1000)/(1 + \Delta^{14}C_z/1000)],$$

where $\Delta^{14}C_S$ is the water $\Delta^{14}C$ at the surface and $\Delta^{14}C_z$ at the depth z in the same column (in permil).

Given the very coarse resolution of our model, we cannot use these simulated reservoir ages to correct any specific $\Delta^{14}C$ reconstruction (like, e.g., applying the reservoir age from Fig. 5b to the Cariaco basin). The only consistent correction we can make is on the simulated atmospheric $\Delta^{14}C$: given that our model predicts reservoir age variations, we can calculate the atmospheric $\Delta^{14}C$ which would be estimated from the sea surface $\Delta^{14}C$ by assuming a constant reservoir age. This is equivalent to producing a synthetic sediment ^{14}C age record, from which we then 'reconstruct' the atmospheric $\Delta^{14}C$ using the standard technique. The difference between this calculated atmospheric $\Delta^{14}C$ (called 'apparent $\Delta^{14}C$' in the following) and the one simulated by the model is the bias due to assuming a constant reservoir age. This calculation can be made for each model box, since the reservoir age varies from box to box. We have made this calculation for the three locations presented in Fig. 5, but only for the simulation with weaker tropical wind for clarity (Fig. 7). Both the phase between atmospheric $\Delta^{14}C$ and reservoir age, and the amplitude of the reservoir age changes, are important in this calculation. In the northern Atlantic, the abrupt drop of this 'apparent $\Delta^{14}C$', at the end of the discharge, is due to the corresponding abrupt increase in the reservoir age. In the tropical Atlantic, the 'apparent $\Delta^{14}C$' varies more abruptly, both for its increase and decrease, getting closer to the reconstruction by Hughen et al. from the Cariaco basin. In the equatorial Pacific, the simulated $\Delta^{14}C$ is amplified but not shifted in time. This shows that, by assuming a constant reservoir age, one might overestimate atmospheric $\Delta^{14}C$ changes.

The 'apparent' atmospheric $\Delta^{14}C$ can increase with a rate up to twice the simulated one, and be 20‰ higher (Table 1), or even of opposite sign (like in the northern Atlantic), due to variations in the reservoir age (about 200 years for the low latitude sites) which are usually within the uncertainty of most studies. This modelling

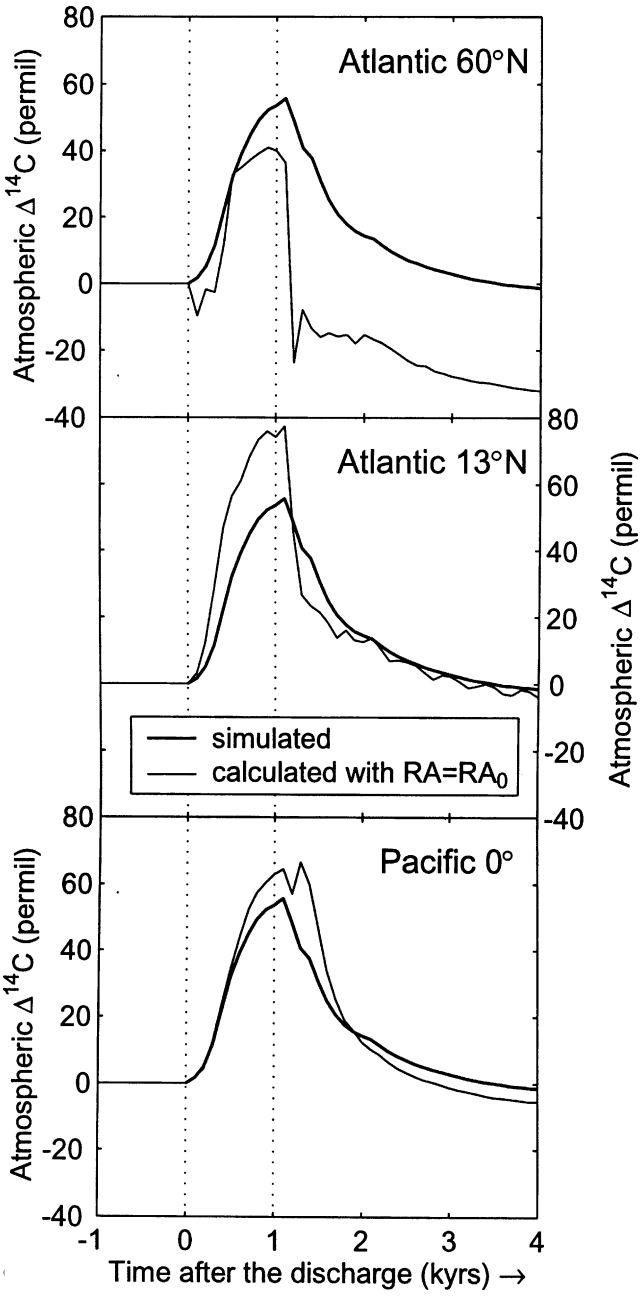

Fig. 7. Apparent atmospheric $\Delta^{14}C$ (plain lines) reconstructed from the simulated sea-surface $\Delta^{14}C$ for the same locations as in Fig. 5, assuming a constant reservoir age (the steady-state reservoir age before the meltwater discharge), compared to the simulated atmospheric $\Delta^{14}C$ (common to all locations; in bold). Only the simulation with weaker tropical wind (plain line in Fig. 3) is shown for clarity. We first calculated the ^{14}C age of the surface water, Age_{c14}, accounting for the changing reservoir age, as (in years):

$$Age_{c14} = Age_{mod} - 8267\log(1 + \Delta^{14}C_{atm}/1000) + RA - RA_0,$$

where RA_0 is the steady-state reservoir age, RA and $\Delta^{14}C_{atm}$ the reservoir age and the atmospheric $\Delta^{14}C$ at model time Age_{mod} (in years). The 'apparent' atmospheric $\Delta^{14}C$, reconstructed from the absolute and ^{14}C age difference ($Age_{mod}-Age_{c14}$) and by assuming $RA = RA_0$, is then (in permil):

$$(\exp[(Age_{mod} - Age_{c14})/8267] - 1)1000.$$

exercise highlights the importance of constraining the reservoir age when trying to reconstruct atmospheric $\Delta^{14}C$ fluctuations.

8. Conclusion

Previous attempts using dynamical models have failed to realistically reproduce the abrupt increase of the atmospheric $\Delta^{14}C$ reconstructed at the onset of the Younger Dryas, casting some doubt on its oceanic origin. Different parameters in such models may explain such a failure. We have investigated the sensitivity of the $\Delta^{14}C$ increase associated to a meltwater discharge to different parameters in a coarse resolution model. The results are summarized in Table 1. The parameter which allows to get closer to the reconstructions is a decrease of the tropical wind. In our simulations, though, the wind stress is not physically coupled to the climatic changes, but only scaled to them. The actual importance of this parameter should be addressed by coupling the wind stress to climatic parameters, i.e., by using climate models of increased complexity. Nonetheless, previous studies have only underlined high- and mid-latitude wind as the most important dynamical feedback during a meltwater discharge (Schiller et al., 1997; Fanning and Weaver, 1997), but the tropics may have a stronger role to play for the atmospheric $\Delta^{14}C$ and climatic variations. The sensitivity of the $\Delta^{14}C$ to the wind and to the rate of meltwater discharge is expected to be reproduced by other models, at least qualitatively. The sensitivity to the vertical diffusivity, K_v, helps explain some earlier GCM results based on models with high vertical diffusivity, but may be less robust because this parameter also influences the oceanic circulation with indirect effects on $\Delta^{14}C$.

When the Atlantic deep overturning collapses, due to a meltwater discharge, the rate of the initial atmospheric $\Delta^{14}C$ increase depends on the rate of this collapse, and thus on the sensitivity of the thermohaline circulation to a surface freshening. An increase of the north Pacific intermediate water formation then plays the stronger role in extending the $\Delta^{14}C$ atmospheric peak, in amplitude and in time. This oceanic response depends on the dynamical and hydrological (through the atmosphere) connections between the basins. The exact balance between these contributions to the atmospheric Δ14C is likely strongly model dependent. Thus, similar studies using models of increased complexity would be useful.

One important advantage of modelling is the prediction of the reservoir age, allowing simulation of ^{14}C fields comparable with measurements. In our simulations, the reservoir age is found to be a critical parameter when reconstructing atmospheric $\Delta^{14}C$ variations. There is indication that the assumption of a

constant reservoir age (within few centuries) might lead to an overestimate of atmospheric $\Delta^{14}C$ amplitude and changing rate.

Acknowledgements

We are grateful to Dr. M. Vellinga for sharing information on their coupled simulation, and to reviewers who helped to improve the manuscript. Discussions with Dr. O. Marchal were very helpful. This study was supported by EC-project POP (Pole-Ocean-Pole, EVK2-CT-2000-00089).

References

Adkins, J.F., Boyle, E.A., 1997. Changing atmospheric $\Delta^{14}C$ and the record of deep water paleoventilation. Paleoceanography 12, 337–344.

Barber, D.C., et al., 1999. Forcing of the cold event of 8,200 years ago by catastrophic drainage of Laurentide lakes. Nature 400, 344–348.

Bard, E., 1998. Geochemical and geophysical implications of the radiocarbon calibration. Geochimica et Cosmochimica Acta 62, 2025–2038.

Bard, E., Arnold, M., Mangerud, J., Paterne, M., Labeyrie, L., Duprat, J., Mélières, M.-A., Sønstegaard, E., Duplessy, J.C., 1994. The North Atlantic atmosphere-sea surface ^{14}C gradient during the Younger Dryas climatic event. Earth and Planetary Science Letters 126, 275–287.

Beaufort, L., de Garidel-Thoron, T., Mix, A.C., Pisias, N.G., 2001. ENSO-like forcing on oceanic primary production during the Late Pleistocene. Science 293, 2440–2444.

Björck, S., 1995. A review of the history of the Baltic Sea, 13.0–8.0ka BP. Quaternary International 27, 19–40.

Broecker, W.S., 1998. Paleocean circulation during the last deglaciation: a bipolar seesaw? Paleoceanography 13, 119–121.

Broecker, W.S., Peteet, D.M., Rind, D., 1985. Does the ocean–atmosphere system have more than one stable mode of operation? Nature 315, 21–26.

Broecker, W.S., Peng, T.-H., Trumbore, S., Bonani, G., Wolfli, W., 1990. The distribution of radiocarbon in the glacial ocean. Global Biogeochemical Cycles 4, 103–117.

Clark, P.U., Marshall, S.J., Clarke, G.K.C., Hostetler, S.W., Licciardi, J.M., Teller, J.T., 2001. Freshwater forcing of abrupt climate change during the last glaciation. Science 293, 283–287.

Clark, P.U., Pisias, N.G., Stocker, T.F., Weaver, A.J., 2002. The role of the thermohaline circulation in abrupt climate change. Nature 415, 863–869.

Duplessy, J.-C., Arnold, M., Bard, E., Juillet-Leclerc, A., Kallel, N., Labeyrie, L., 1989. AMS ^{14}C study of transient events and of the ventilation rate of the Pacific Intermediate Water during the last deglaciation. Radiocarbon 31, 493–502.

Esbensen, S.K., Kushnir, Y., 1981. The Heat Budget of the Global Ocean: an Atlas based on estimates from surface marine observations. Report no. 29. Climatic Research Institute, Oregon University, Corvallis.

Fairbanks, R.G., 1989. A 17,000-year glacio-eustatic sea level record: influence of glacial melting rates on the Younger Dryas event and deep-ocean circulation. Nature 342, 637–642.

Fanning, A.F., Weaver, A.J., 1997. Temporal-geographical meltwater influences on the North Atlantic Conveyor: implications for the Younger Dryas. Paleoceanography 12, 307–320.

Hughen, K.A., Southon, J.R., Lehman, S.J., Overpeck, J.T., 2000. Synchronous radiocarbon and climate shifts during the Last Deglaciation. Science 290, 1951–1954.

Joos, F., Orr, J.C., Siegenthaler, U., 1997. Ocean carbon transport in a box-diffusion versus a general circulation model. Journal of Geophysical Research 102, 12,367–12,388.

Jouzel, J., and 11 others, 1995. The two-step shape and timing of the last deglaciation in Antarctica. Climate Dynamics 11, 151–161.

Loubere, P., 1999. A multiproxy reconstruction of biological productivity and oceanography in the eastern equatorial Pacific for the past 30,000 years. Marine Micropaleontology 37, 173–198.

Manabe, S., Stouffer, R.J., 1995. Simulation of abrupt climate change induced by freshwater input to the North Atlantic ocean. Nature 378, 165–167.

Manabe, S., Stouffer, R.J., 1997. Coupled ocean–atmosphere model response to freshwater input: comparison to Younger Dryas event. Paleoceanography 12, 321–336.

Marcantonio, F., Anderson, R.F., Higgins, S., Fleisher, M.Q., Stute, M., Schlosser, P., 2001. Abrupt intensification of the SW Indian Ocean monsoon during the last deglaciation: constraints from Th, Pa, and He isotopes. Earth and Planetary Science Letters 184, 505–514.

Marchal, O., Stocker, T.F., Joos, F., Indermühle, A., Blunier, T., Tschumi, J., 1999. Modelling the concentration of atmospheric CO_2 during the Younger Dryas climate event. Climate Dynamics 15, 341–354.

Marchal, O., Stocker, T.F., Muscheler, R., 2001. Atmospheric radiocarbon during the Younger Dryas: production, ventilation, or both? Earth and Planetary Science Letters 185, 383–395.

Mikolajewicz, U., 1996. A meltwater induced collapse of the 'conveyor belt' thermohaline circulation and its influence on the distribution of $\Delta^{14}C$ and $\delta^{18}O$ in the oceans. Report no. 189, Max-Planck-Institut für Meteorologie, Hamburg.

Mikolajewicz, U., Crowley, T.J., Schiller, A., Voss, R., 1997. Modelling teleconnections between the North Atlantic and North Pacific during the Younger Dryas. Nature 387, 384–387.

Muscheler, R., Beer, J., Wagner, G., Finkel, R.C., 2000. Changes in deep-water formation during the Younger Dryas event inferred from ^{10}Be and ^{14}C records. Nature 408, 567–570.

Rind, D., 1998. Latitudinal temperature gradients and climate change. Journal of Geophysical Research 103, 5943–5971.

Rind, D., Russell, G.L., Schmidt, G.A., Sheth, S., Collins, D., deMenocal, P., Teller, J., 2001. Effects of glacial meltwater in the GISS coupled atmosphere-ocean model 2. A bipolar seesaw in Atlantic Deep Water production. Journal of Geophysical Research 106, 27,355–27,366.

Schiller, A., Mikolajewicz, U., Voss, R., 1997. The stability of the North Atlantic thermohaline circulation in a coupled ocean–atmosphere general circulation model. Climate Dynamics 13, 325–347.

Schmittner, A., Appenzeller, C., Stocker, T.F., 2000. Validation of parametrisations for the meridional energy and moisture transport used in simple climate models. Climate Dynamics 16, 63–77.

Seidov, D., Haupt, B.J., 1997. Global ocean thermohaline conveyor at present and in the late Quaternary. Geophysical Research Letters 24, 2817–2820.

Siani, G., Paterne, M., Michel, E., Sulpizio, R., Sbrana, A., Arnold, M., Haddad, G., 2001. Mediterranean Sea Surface Radiocarbon Reservoir Age changes since the Last Glacial Maximum. Science 294, 1917–1920.

Siegenthaler, U., Heimann, M., Oeschger, H., 1980. ^{14}C variations caused by changes in the global carbon cycle. Radiocarbon 22, 177–191.

Stocker, T.F., Wright, D.G., 1991. Rapid transitions of the ocean's deep circulation induced by changes in surface water fluxes. Nature 351, 729–732.

Stocker, T.F., Wright, D.G., 1996. Rapid changes in ocean circulation and atmospheric radiocarbon. Paleoceanography 11, 773–795.

Stocker, T.F., Wright, D.G., Mysak, L.A., 1992. A zonally averaged, coupled ocean–atmosphere model for paleoclimate studies. Journal of Climate 5, 773–797.

Stuiver, M., Polach, H.A., 1977. Discussion: reporting of ^{14}C data. Radiocarbon 19, 355–363.

Toggweiler, J.R., Dixon, K., Bryan, K., 1989. Simulations of radiocarbon in a Coarse-Resolution World Ocean Model 1. Steady state prebomb distributions. Journal of Geophysical Research 94, 8217–8242.

van Geen, A., Fairbanks, R.G., Dartnell, P., McGann, M., Gardner, J.V., Kashgarian, M., 1996. Ventilation changes in the northeast Pacific during the last deglaciation. Paleoceanography 11, 519–528.

Vellinga, M., Wood, R.A., 2001. Global climatic impacts of a collapse of the Atlantic thermohaline circulation. Report no. 26, Hadley Centre technical note, Hadley Centre for Climate Prediction and Research, Bracknell.

Waelbroeck, C., Duplessy, J.-C., Michel, E., Labeyrie, L., Paillard, D., Duprat, J., 2001. The timing of the last deglaciation in North Atlantic climate records. Nature 412, 724–727.

Wanninkhof, R., 1992. Relationship between wind speed and gas exchange over the ocean. Journal of Geophysical Research 97, 7373–7382.

Wright, D.G., Stocker, T.F., 1992. Sensitivities of a zonally averaged global ocean circulation model. Journal of Geophysical Research 97, 12707–12730.